16
Photoreactors

Roger Gorges and Andreas Kirsch

16.1
Photochemical Reactions

Photochemical reactions comprise chemical reactions for which the required activation energy is provided by incident light rather than by heat. In order for photochemical reactions to proceed, light photons must be absorbed either directly by the substrate molecule or by a photosensitzer/photocatalyst, which then transfers the reaction energy to the substrate molecule. Because only discrete quanta of energy can be absorbed, the energy of the illuminating light, i.e. its wavelength, must correspond to the absorption wavelength of the substrate molecule or the photosensitizer/photocatalyst. Photochemical reactions still remain a small area of preparative organic chemistry, with industrial scale-up being fairly difficult. Nonetheless, a number of advantages can be attributed to the use of photochemical reactions [1]:

1. Light may be considered as a highly specific and ecologically clean "reagent".
2. Photochemical methods offer less "aggressive" routes in chemical synthesis than thermal methods.
3. Photochemical reactions may contribute to the safety of industrial processes, because they are generally performed at or below room temperature.
4. Photochemically reacting organic compounds do not require any protecting groups.
5. Many conventional syntheses can be shortened by inserting photochemical steps.

Photochemical reactions in microstructured reactors have not been investigated in-depth so far and only a few reaction examples exist in the literature [2]. The different existing studies, however, quote similar advantages associated with carrying out photochemical reactions in microstructures.

Many photoreactions proceed via a radical chain reaction mechanism. In these reactions, reactive radical species are formed in the vicinity of the light source and must be transported subsequently to the place of reaction, where they interact with the substrate molecule. Generally, the transport of the radicals takes place by

Micro Process Engineering, Vol.1: Fundamentals, Operations and Catalysts
Edited by V. Hessel, A. Renken, J.C. Schouten, and J.-I. Yoshida

ISBN: 978-3-527-31550-5

diffusion. If transport is not fast enough, radicals can recombine, which represents a strongly exothermic reaction, additionally heating the reaction mixture locally. Furthermore, each radical recombination decreases the quantum yield and thus the efficiency of the reaction regime. Microstructures, with their advantageous surface-to-volume ratio and their small dimensions, have short diffusion paths and therefore increase the likelihood of radicals interacting with substrate molecules. Hence quantum yields of photochemical reactions can be enhanced significantly. Due to the microscale dimensions, short residence times and excellent heat transfer characteristics are achieved, which avoid undesirable side reactions.

Another problem with technical photochemical reactors is the individual absorption of reactants and solvents. If batch-type reactors with immersion lamps are employed, only a small film in the vicinity of the lamp is irradiated in solutions with high molar extinction coefficients. Light intensity decreases exponentially with distance to the light source, according to the Beer–Lambert law. In reaction engineering, this drawback is sometimes compensated by the use of falling film reactors or spray towers in order to achieve very thin fluid films by skillful fluid management. If photochemical reactions are carried out in microstructured reactors, the irradiated fluid film is determined by the geometry of the microstructure, which generally has a depth of only a few micrometers. Hence in microstructures, highly absorbing solutions, i.e. solutions with high concentrations, can be handled easily. Due to the small dimensions, complete penetration of the entire reaction solution can be achieved, which leads to a significant increase in the quantum yield of the reaction and an improvement in the reaction engineering efficiency.

Table 16.1 gives an overview of photochemical reactions in microstructures that have been reported in the literature.

In the following sections, the different reaction types are discussed exemplarily and advantages associated with carrying out these reactions in microstructures are explained in detail. Reactions are classified into three categories according to the number and type of phases involved in the reaction: single-phase reactions, multiphase reactions and reactions on the surface of an immobilized photocatalyst.

16.2 Single-phase Photochemical Reactions

Single-phase photochemical reactions or homogeneous photochemical reactions take place in the liquid phase in most cases. The substrate molecules are often dissolved in an organic solvent and in some cases an additional photosensitizer is also dissolved. This reaction category was amongst the first to be investigated in microreactors.

In a pioneering work in 2001, Lu *et al.* demonstrated the photochemical coupling of benzophenone molecules to benzopinacol [3]. Isopropyl alcohol acts as both a solvent and a reducing agent (Scheme 16.1).

The pinacol coupling reaction is investigated in two different microreactors. In one reactor the detection with UV–visible spectroscopy is performed on a separate in-line

Table 16.1 Photochemical reactions in microstructured reactors.

No.	Reaction	Microreactor	Light source	Reference
Single-phase photochemical reactions				
1	Pinacol coupling	Si–Pyrex/Si–quartz	JKL Mini UV lamp	[3]
2	Intramolecular [2 + 2] photocycloaddition of 1-cyanonaphthalene	PDMS (polydimethylsiloxane) microchannel reactor	Xenon lamp	[4]
3	[2 + 2] Photochemical cycloaddition of cyclohexenone	Foturan glass microchannel reactor	300 W high-pressure mercury lamp	[6]
4	Nitrite photolysis (Barton reaction)	Pyrex glass-covered stainless-steel microreactor	15 W black light lamp (352 nm)	[7]
5	Photodegradation of Cu–EDTA complexes	Polycarbonate microchannel reactor	10 mW UV-LED (Nichia, 365 nm)	[8]
6	Photosensitized oxidation of citronellol in microreactors	High temperature-resistant Borofloat glass meandering microchannel	LEDs (Kingbright, 468 nm)	[9]
7	Photocycloaddition of 2-(2-alkenyloxy-methyl)naphthalene-1-carbonitriles	Pyrex glass microchannel reactor	Xenon lamp	[5]
Multi-phase photochemical reactions				
8	Photooxygenation with singlet oxygen	Glass microchannel reactor	20 W tungsten microscope lamp	[10]
9	Photochlorination of alkyl aromatics	Pyrex glass-covered stainless-steel falling film reactor	1000 W xenon lamp	[11]
10	[4 + 2] Cycloaddition of 2-cyclopentene-1.4-diol	Pyrex glass-covered stainless-steel falling film reactor	Xenon lamp	[12]
11	Photocyanation of pyrene	Polystyrene microchannel reactor	300 W mercury lamp	[13]

(*Continued*)

Table 16.1 (*Continued*)

No.	Reaction	Microreactor	Light source	Reference
Immobilized photocatalyst				
12	Photodegradation of 4-chlorophenol	TiO_2-coated LTCC ceramic microchannel reactor	UV-LEDs (385 nm)	[14]
13	Photodegradation of phenol	Polystyrene/Teflon microchannel chip	300 W high-pressure mercury lamp	[15]
14	Photocatalytic reduction of benzaldehyde and nitrotoluene	TiO_2-coated quartz glass microchannel reactor	UV LEDs (365 nm)	[16]
15	*N*-Alkylation of benzylamine in ethanol	TiO_2-coated quartz glass microchannel reactor	UV-LEDs	[17]
16	Photocatalytic characteristics on sintered glass and microreactor	Borosilicate sintered glass microchannel reactor	15 W UV lamp ($\lambda < 380$ nm)	[18]
17	Photodegradation of methylene blue	Soda-lime wafers	Combined mercury–xenon arc lamp	[19]
18	Photodegradation of methylene blue	Microchannel ceramic disk	High-pressure mercury lamp	[20]

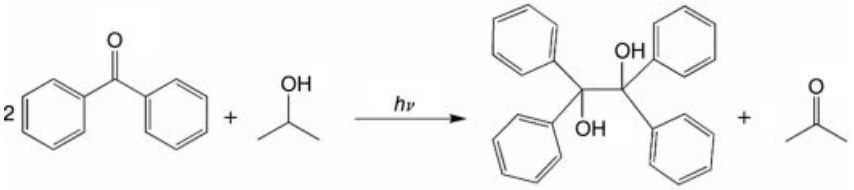

Scheme 16.1 Reductive photochemical coupling of benzophenone to benzopinacol.

detection chip (hybrid solution) and in another reactor the detection is effected directly on the microchip (monolithic solution). Results from on-line spectroscopy can in principle be confirmed by HPLC measurements; however, it is observed that a dark reaction contributes to an additional increase in yield. *In situ* monitoring of the monolithic solution has been found to be difficult because reaction intermediates show strong absorption in the same wavelength region as the educts to be measured. Analysis of the quantum yield of the reaction in relation to the flow rate employed, corresponding to the residence time on the chip, show that quantum yield increases with increasing flow rate and finally surpasses the quantum yields reported in the literature for conventional reaction engineering. The authors explain this behavior with the decrease in the extinction of the reaction mixture due to the formation of the non-absorbing product benzopinacol. Hence fewer light quanta are absorbed and pass through the reaction mixture without initiating a reaction. No measurable conversion is found for flow rates higher than $10\,\mu L\,min^{-1}$. Residence times at higher flow rates do not suffice for radicals formed in the vicinity of the light source to diffuse into the reaction mixture. Flow rates lower than $3\,\mu L\,min^{-1}$ lead to the crystallization of benzopinacol on the microchip.

Maeda *et al.* examined intramolecular [2 + 2] photocycloadditions of 1-cyanonaphthalene derivatives (**I**) in microchannel reactors [4]. They use microreactors made of polydimethylsiloxane (PDMS) and Pyrex glass. With a photolithographic method, channels of 300 µm width, 50 µm depth and 45–202 mm length are fabricated. For the photoreaction (Scheme 16.2), flow rates of $0.03–0.005\,mL\,h^{-1}$ are applied and a xenon lamp with a UV-29 filter (> 290 nm) is used as a light source. The authors report that under the conditions prevailing in the microreactor, higher regioselectivity and efficiency are achieved compared with batch process conditions.

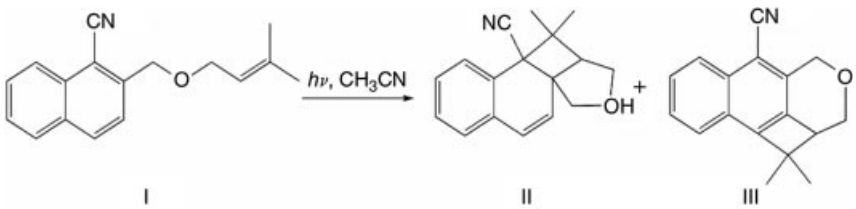

Scheme 16.2 Intermolecular [2 + 2] photocycloaddition of 1-cyanonaphthalene derivatives.

Thus, ~50% yields of the target product (**II**) are obtained for irradiation times of 1–5 min, whereas under batch conditions the yields amount only to 5%. In order to observe similar yields in the batch reactor, reaction times of >180 min are required. Due to the possible photocycloreversion of 1-cyano-5-oxabenzo [10, 11] tricycle [5.4.0.0]undec-8-ene (**I**), a prolonged irradiation yields the secondary product (**III**). The authors attribute an increase in regioselectivity to the specific flow system of the microreactor.

Recently, Mukae *et al.* demonstrated the intermolecular [2 + 2] and [2 + 3] photocycloadditions of 2-(2-alkenyloxymethyl)naphthalene-1-carbonitriles using microchannel reactors made of Pyrex glass [5]. Channel dimensions are 100 µm width, 40 µm depth and 120 mm length. The flowing solution is irradiated with a xenon lamp. Irradiation times in the range of 9–172 s and flow rates of 0.03 mL h^{-1} are applied Analyses are carried out using NMR spectroscopy. In comparison with a batch system, similar conversion yields of the educts are obtained. However, in the microreactor system higher regioselectivity of the products can be achieved (product ratio **II**:**III**: batch system 55:45, microreactor system 96:4). The authors report that by increasing the width of the microchannels from 100 to 2500 µm, a 25-fold higher quantity of the products can be achieved. The residence times in both microchannel systems are similar and a comparable regioselectivity is obtained. However, the increase in products is attributed to the higher interfacial surface area exposed to the light source.

Fukuyama's group also investigated [2 + 2] photocycloadditions [6]. Cyclohex-2-enone derivatives and vinyl acetate interact under UV irradiation to give bicylcooctanone derivatives (Scheme 16.3). As a microreactor, a microchannel device made of Foturan glass with a depth of 500 µm, a width of 1000 µm and a length of 1.4 m is applied. The reactor itself consists of two channels, one channel being used as a heat exchanger and the other for the photoreaction. At a flow rate of 0.5 mL h^{-1} and a residence time of 2 h in the microreactor device, a yield of 88% of the desired product can be achieved, whereas after an irradiation of 2–4 h under batch conditions, yields of only 8–22% are obtained. Hence the reaction rate increases rapidly under microreactor conditions. An additional stacking of multiple microreactor devices allows for even higher flow rates.

Another interesting photochemical transformation conducted in a microreactor was examined by Sugimoto *et al.* [7]. A continuous flow microreactor is used to

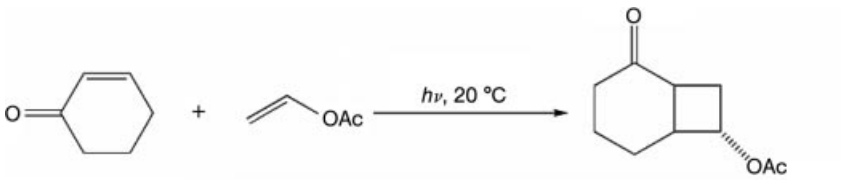

Scheme 16.3 [2 + 2] Photocycloadditions of cyclohex-2-enone derivatives.

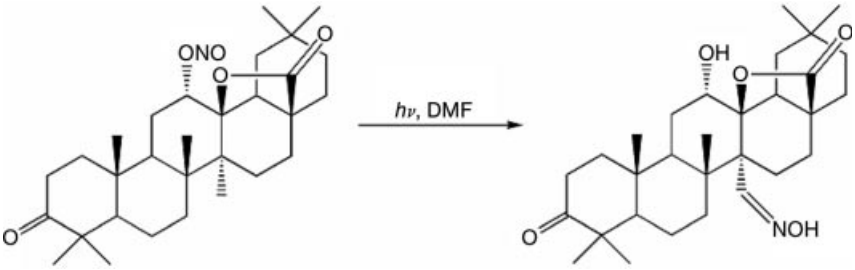

Scheme 16.4 Barton nitrite photolysis of a steroidal compound.

synthesize a steroid intermediate for an endothelin receptor antagonist. The synthesis follows the Barton reaction and takes place in a glass-covered stainless-steel microreactor. In the Barton reaction, remote functionalization of saturated alcohols takes place by the use of photoirradiation conditions for nitrite esters (Scheme 16.4). The nitrite esters are prepared from the corresponding alcohols with nitrosyl chloride.

The microchannel dimensions used for the synthesis have an average width of 1000 μm, a depth of 500 μm and total length of 1 m. Eight 15 W black light lamps with a maximum peak wavelength of 352 nm are employed as light sources. The microreactor has a hold-up volume of 8 mL. After 20 h of continuous flow, ~3 g of the desired product are obtained (60% yield). Products are analyzed by an HPLC method and purified by silica gel column chromatography. Multi-gram scale production is achieved by using two serial multi-lane microreactors.

Meyer *et al.* examined the formation of rose oxide by the oxidation of citronellol with singlet oxygen in a temperature-resistant glass (Borofloat) microreactor [9]. A 10 mL β-citronellol–ethanol solution with $Ru(^tbpy)_3Cl_2$ is circulated through the microchannel reactor (hold-up volume 0.27 mL). Products are identified by HPLC analysis. After an irradiation time of 40 min, space–time yields of 0.8 mmol L^{-1} min^{-1} are obtained. In a comparable batch process, space–time yields are ~10 times lower.

16.3
Multi-phase Photochemical Reactions

Multi-phase photochemical reactions take place across phase boundaries. In most cases, substrate molecules are either dissolved in different liquid phases or one reactant is in the gas phase and interacts with the liquid phase. For this reaction category, phase transfer kinetics, in addition to the actual photochemical reaction, have to be taken into account, assuming microreactors to be ideal reaction engineering tools due to their low mass transfer limitations.

An early example of a multi-phase microreaction was reported by Wootton *et al.*, who demonstrated the continuous photochemical production of singlet oxygen and its use in organic synthesis for the cyclooxidation of α-terpinene to ascaridol (Scheme 16.5) [10].

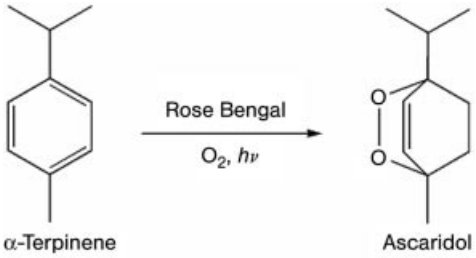

Scheme 16.5 Photochemical generation of singlet oxygen and oxygenation of α-terpinene to ascaridol.

Oxygen saturation of the solvent methanol is achieved immediately prior to the reaction by introducing the gas into the liquid phase via a Y-mixer that is directly integrated on the chip. In this way, the amount of oxygenated solvent can be limited to a few picoliters, which leads to a significant improvement in reaction safety. In large-scale technical systems, the handling of oxygenated solvents is regarded as extremely difficult and dangerous. Rose Bengal is used as a photosensitizer. Despite its high molar extinction coefficient of 99 800 $cm^{-1}\,M^{-1}$ at 550 nm, the transmission through a 5×10^{-3} M solution is still 95% because the optical pathlength inside the microreactor is only 50 µm. Yields of >80% can be achieved for reactions times of less than 5 s.

Ehrich *et al.* investigated the photochlorination of the side-chain of an alkyl aromatic compound using the example of the conversion of toluene-2,4-diisocyanate (TDI) to 1-chloromethyl-2,4-diisocyanatobenzene (1Cl-TDI) [11]. The reaction product represents an important intermediate in the production of polyurethane. The ring chlorination to toluene-5-chloro-2,4-diisocyanate (5Cl-TDI) occurs as a secondary reaction (Scheme 16.6). The main product and secondary product can react further to give high molecular weight resultant products.

The reaction, which proceeds at the gas–liquid interface, is carried out in a falling film microreactor (IMM, Mainz, Germany). The liquid phase (TDI in tetrachloroethane) is passed as a falling film through the microstructure from top to bottom while the gas phase (chlorine) is passed countercurrent from bottom to top (Figure 16.1). The material of the microstructure in which the reaction takes place is varied between nickel and iron in order to investigate the influence of the formation of the Lewis acid $FeCl_3$ under the reaction conditions. For reasons of comparison, the same reaction is carried out in a batch reactor. It can be shown that, compared with the batch reactor, in the microreactor a two times higher selectivity towards the target product 1-Cl-TDI can be obtained. The calculated space–time yield increases by more than two orders of magnitude from 1.3 mol $L^{-1}\,h^{-1}$ for the batch reactor to 401 mol $L^{-1}\,h^{-1}$ for the falling film microreactor. The authors explain the increase in selectivity with the fact that in the microreactor the concentration of chlorine radicals can be kept lower due to its large surface-to-volume ratio. In the microreactor, the entire fluid film can be penetrated by the incident light, in contrast to the batch reactor, where only a thin film of the fluid is irradiated in the vicinity of the light

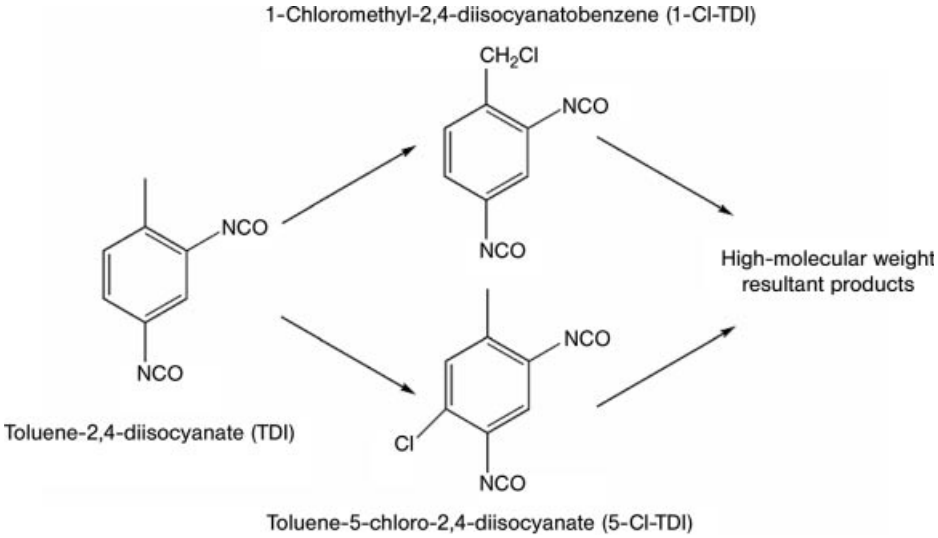

Scheme 16.6 Photochlorination of toluene-2,4-diisocyanate (TDI) to the target product 1-chloromethyl-2,4-diisocyanatobenzene. As a secondary product toluene-5-chloro-2,4-diisocyanate is formed.

source. As a consequence, only a few substrate molecules are excited and the ring chlorination is preferred, which explains the decrease in selectivity towards 1-Cl-TDI. Furthermore, it can be shown that no mass transport limitation prevails for the transfer of chlorine from the gas phase into the liquid phase and thus intrinsic kinetic data can be readily extracted for the investigated reaction network.

With a similar microreactor, a photoinduced [4 + 2]-cycloaddition was carried out by Jähnisch [12]. 2-Cyclopentene-1,4-diol is formed through the reaction of

Figure 16.1 Falling film reactor (IMM).

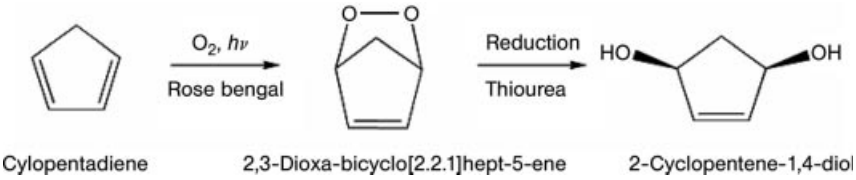

Scheme 16.7 Photochemical generation of singlet oxygen and oxygenation of cyclopentadiene to 2-cyclopentene-1,4-diol.

pentadiene with singlet oxygen, as shown in Scheme 16.7. Due to the minimal holdup of the microreactor, the explosive intermediate generated does not cause any safety risks. The reaction takes place in a microreactor with 32 parallel channels (600 µm width, 300 µm depth and 66 mm length). Yields of ~20% are obtained with feed flows of 1 mL min^{-1} for the liquid phase and 15 L h^{-1} for oxygen.

The photocyanation of pyrene in a microchannel through an oil–water interface was investigated by Ueno *et al.* [13]. The microchips employed are made of polystyrene by embossing with a silicone template. The phase transfer reaction proceeds in four steps as depicted in Figure 16.2. In the first step, a photoinduced electron transfer in the oil phase (polycarbonate) occurs from the aromatic hydrocarbon pyrene (DH) to the electron acceptor 1,4-dicyanobenzene (A). The cationic $DH^{\bullet+}$ radical is subsequently the target of the nucleophilic attack of the cyanide anion at the oil–water interface. The cyanated product DCN is insoluble in water and goes back into the oil phase. Experiments without a cyanide source (NaCN) in the aqueous phase show no reaction. Hence it can be excluded that the nucleophilic-substituted cyanide originates from the electron acceptor 1,4-dicyanobenzene.

With the reaction setup described in Figure 16.2, a flow rate of 0.2 µL min^{-1} and a residence time of 210 s, a DCN yield of 28% can be attained. Furthermore, it can be shown that the yield decreases linearly with decreasing residence time or increasing

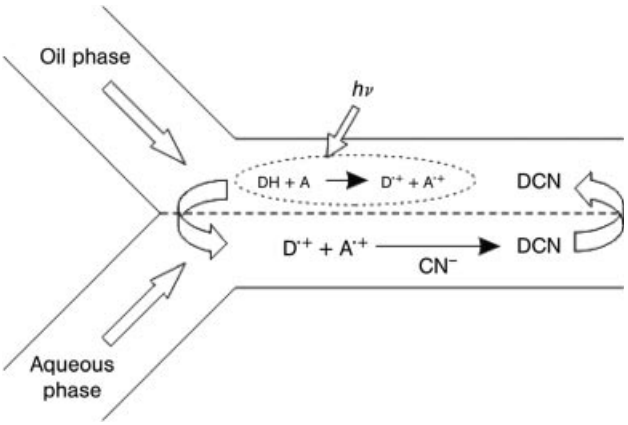

Figure 16.2 Photocyanation across a phase boundary. Adapted from [13].

flow rate. Since yield is predominantly determined by the size of the oil–water interface, a double-Y chip is produced in a second experiment, in which three stable liquid lamellae flow concurrently in the microchannel. The ratio of the oil–water interface to the oil phase volume is three times higher than that of the two-lamella chip. With this chip, a yield of 73% can be achieved for the same flow rate and residence time. Flow rates below $0.2\,\mu L\,min^{-1}$ do not result in a stable oil–water interface.

16.4 Immobilized Photocatalysts

Photocatalytic reactions in microstructured reactors represent yet another level of complexity since a solid catalyst (e.g. TiO_2) must be immobilized on the microstructure, in addition to the other general requirements of photomicroreactors. In contrast to batch systems, which mainly use suspensions of dispersed powders, in microstructured devices this would result in technical difficulties due to plugging or blocking of the microchannels. Therefore, the immobilization of the solid photocatalyst is a quintessential requirement if heterogeneous photocatalytic reactions are carried out in microreactors. The immobilization of the photocatalyst can be achieved in multiple ways; e.g. Kitamori's group [21] investigated the use of sol–gel methods, Miguez *et al.* [22] utilized CVD (chemical vapor deposition) procedures and colloidal crystal methods were investigated by Nakamura *et al.* [23] and by Wootton's group [19].

Gorges *et al.* described the immobilization of a photocatalytically active titanium dioxide catalyst by anodic spark deposition [14]. Figure 16.3 depicts a cross-section through a microchannel that has been coated in this fashion with a TiO_2 layer.

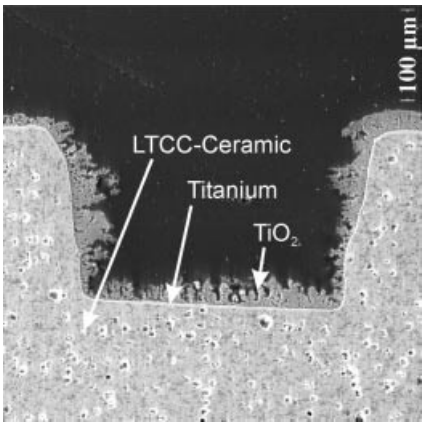

Figure 16.3 SEM cross-section of microchannel coated with TiO_2 photocatalyst. Adapted from [14].

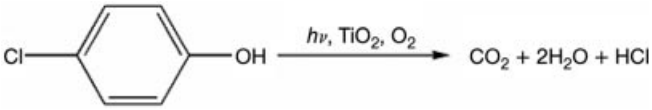

Scheme 16.8 Photodegradation of 4-chlorphenol.

Illumination of this coated microstructure is achieved by UV-A light-emitting diodes (385 nm). As a model reaction, the authors investigate the degradation of 4-chlorophenol (Scheme 16.8).

The reaction progress is monitored off-line by HPLC. Flow rates, residence times and initial concentrations of 4-chlorophenol are varied and kinetic parameters are calculated from the data obtained. It can be shown that the photocatalytic reaction is governed by Langmuir–Hinshelwood kinetics. The calculation of Damköhler numbers shows that no mass transfer limitation exists in the microreactor, hence the calculated kinetic data really represent the intrinsic kinetics of the reaction. Photonic efficiencies in the microreactor are still somewhat lower than in batch-type slurry reactors. This finding is indicative of the need to improve the catalytic activity of the deposited photocatalyst in comparison with commercially available catalysts such as Degussa P25 and Sachtleben Hombikat UV 100. The illuminated specific surface area in the microchannel reactor surpasses that of conventional photocatalytic reactors by a factor of 4–400 depending on the particular conventional reactor type.

Kitamura *et al.* examined the photodegradation of phenol by a silica-supported porphyrin derivative in polymer microchannel chips [15]. With an imprinting method, they fabricate dam-structured microchannel chips. The channels are filled with silica gel particles, which are modified with monopyridyltriphenylporphyrin (PyTPP). The Si–PyTPP particles act as photosensitizers (Scheme 16.9).

The stated reaction pathway is the photodecomposition of phenol via a singlet oxygen mechanism. Kitamura *et al.* used a 300 W high-pressure mercury lamp (1.0 M

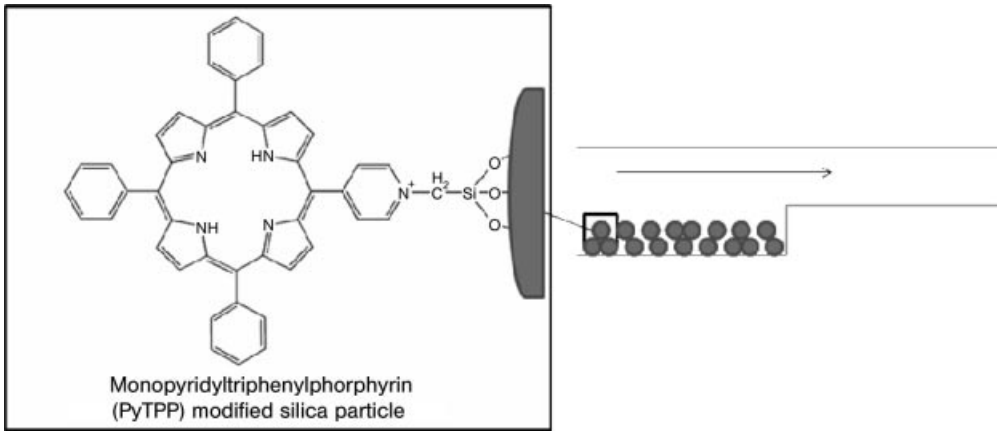

Scheme 16.9 Silica gel particles modified with monopyridyltriphenylporphyrin (PyTPP). Adapted from [15].

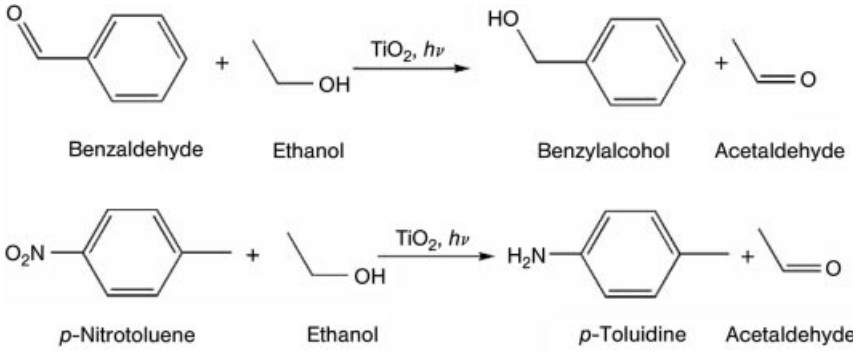

Scheme 16.10 Photoreduction of benzaldehyde and nitrotoluene.

$CuSO_4$ solution filter, $\lambda > 330$ nm) as a light source. They achieve phenol photodecomposition yields as high as 93% at solution flow rates of 0.5 L min^{-1} with a reaction time of 42 s, whereas under similar conditions in a bulk reactor the PyTPP–SiO_2 suspension provides yields of only 73% with reaction times of ~2 h.

Matsushita's group described the photocatalytic reduction of benzaldehyde and nitrotoluene in quartz microreactors with titanium dioxide as photocatalyst [16]. They use microchannels of 500 μm width, 100 μm depth and 40 mm length. The bottom and the walls of the channel are coated with titanium dioxide to achieve an illuminated specific surface area of 1.4×10^4 m^2 m^{-3}. Benzaldehyde or nitrotoluene are dissolved in different alcoholic solutions and introduced into the microreactor by a syringe pump. UV-LEDs with a peak wavelength of 365 nm are utilized as light sources. The photocatalytic reduction is shown in Scheme 16.10. After excitation of TiO_2, the electron hole formed can oxidize the alcoholic media, whereas the reduction is initiated by electron transfer from TiO_2 to benzaldehyde or nitrotoluene. The authors report increasing reduction with increase in residence time. An irradiation time of 60 s yields 45% of *p*-toluidine and 10.7% of benzyl alcohol.

In addition, Matsushita *et al.* investigated the *N*-alkylation of benzylamine in ethanol [17]. Microreactors consisting of quartz with a microchannel of 500 μm width and 500 μm depth are employed for the reaction. The channel is coated with titanium dioxide or Pt-loaded titanium dioxide as photocatalyst. UV light-emitting diodes with a peak wavelength of 365 nm are used as excitation light source. The authors observe yields of 40% for the Pt-free TiO_2 and 85% with TiO_2/Pt as photocatalyst. The residence time is 150 s (Scheme 16.11).

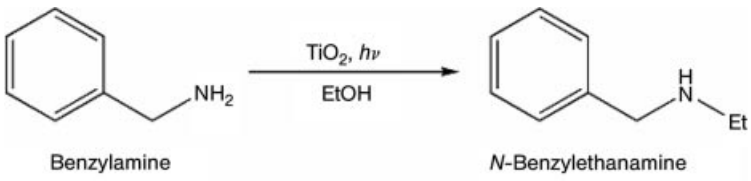

Scheme 16.11 Ethylation of benzylamine.

Another photodegradation reaction was investigated by Choi *et al.* [18]. They use a sintered glass reactor and a microchannel reactor to compare the degradation of D-glucose. Each microchannel has a diameter of 800 µm and a length of 1 m. Both reactor types have a maximum feed stream of 10 mL min^{-1}. Titanium dioxide is used as photocatalyst and applied in a wash coating procedure with a solution of hydrolyzed titanium oxysulfate. The examined photodegradation of D-glucose follows the Langmuir–Hinshelwood mechanism and is completely controlled by the catalyst surface reaction. On condition that the titanium dioxide loading in both reactors is identical, the microchannel reactor provides better degradation results than a sintered-glass reactor.

Recently, Wootton's group demonstrated the photodegradation of methylene blue on titanium dioxide surfaces in microreactors [19]. The microdevices are produced by laser lithography of soda-lime glass wafers. The fabricated microstructure consists of a serpentine channel (50 µm depth, 2.97 µL holdup volume) subdivided into 11 rows with additional 32 side lobes per row. The reactor itself has two inlets – one for the gas phase and the other for the liquid phase. For the photocatalyst coating, an 11% titanium dioxide suspension is filled in the microstructures and the excess suspension is flushed out with nitrogen. Subsequently, the devices are heated at 400 °C for 6 h to obtain a 1 µm thick titanium dioxide layer. A combined mercury and xenon arc lamp is used as the light source. The projected area averages 0.53 cm^2. The reactant solutions are analyzed using absorption spectroscopy. The authors report that, by irradiation of an aerated methylene blue solution in the coated micro chip, conversion rates of 0.63% s^{-1} can be achieved. By introducing additional gaseous oxygen into the microchannel, significantly higher conversion rates (3.33% s^{-1}) are obtained. The authors state that because the solubility of oxygen is relatively low in aqueous systems and because of the small confined space within a microreactor, rapid depletion of the dissolved oxygen occurs. Hence additional gaseous oxygen greatly increases the photodegradation.

Teekateerawej *et al.* also investigated the photodegradation of methylene blue [20]. They use porous alumina ceramic disks as microchannel reactors. The disks are dip-coated with two titanium dioxide solutions to provide different roughnesses of the catalyst surface. One microdisk has about 1250 microchannels, each of 50 µm diameter and 200 µm length. A 250 W high-pressure mercury lamp is used as the light source. The photocatalytic reaction is evaluated by measuring the absorbance of the methylene blue solution. With flow rates ranging from 1.3 to 11.4 cm^3 min^{-1} and irradiation times of 1–180 min, decomposition yields of ~30–40% can be achieved. The authors report that the reaction mechanism is subject to pseudo-first-order kinetics and that an additional oxygen gas stream increases the photodegradation significantly. Furthermore, they observe a decrease in the reaction rate at higher flow rates and with rougher surface areas. The authors propose that high flow rates in connection with rough surface areas can build up stagnation layers near the microchannel walls and therefore constrain the lateral mass transfer, which leads to decreased photocatalytic activity. Consequently, smoother microchannel surfaces favor higher flow rates.

16.5 Conclusion

Different types of microreactors, ranging from single-channel to multi-channel designs, and even more complex falling film reactors, have been investigated for carrying out photochemical reactions. Reported channel dimensions of photomicroreactors range from 10 to 1000 μm.

Due to their inherent superior process control capabilities (precise flow rate, residence time, etc.), photomicroreactors proved to be a powerful tool in reaction engineering if secondary or consecutive reactions must be minimized.

Although in all cases emphasis is put on the miniaturization of the chemical reactor itself, the light sources required are not always similarly reduced in size. Hence irradiation is still often carried out with macroscopic xenon or mercury lamps, which have high energy consumption and an unfavorable electric power to light power conversion efficiency. Furthermore, their light beam is usually not exclusively focused on the reaction space and therefore is most often not applied very efficiently. As a consequence, these macroscopic light sources may contribute significantly to heating of the microstructure and the reaction mixture. This has to be prevented, e.g. by the integration of micro heat exchangers in order to avoid undesired thermal side or consecutive reactions, which could lower the reaction yield. UV-LEDs as miniaturized light sources recently emerged on the market and represent a promising tool for further developments in the field of photomicroreactors. Whereas today's UV-LEDs emit light in the UV-A range of ~365 nm, new generations of UV-LEDs might emit in the UV-B or even the UV-C range, allowing for the excitation of an even broader range of substrate molecules.

Even though the output of a single microdevice can be increased by connecting many devices in parallel, no concept has yet been presented for numbering-up or stacking-up of photomicroreactors comparable to those concepts tested for conventional thermal microreactors. This might be due to the difficulties associated with providing light to a multitude of microchannels.

All photocatalytic reactions are carried out with an immobilized heterogeneous photocatalyst. Slurries are difficult to handle in microstructures and often lead to clogging problems. Immobilized catalysts in microstructures, however, have the advantage that no separation from the reaction mixture in an additional costly and time-intensive separation step is required as for conventional slurry-type batch reactors. In contrast to conventional immobilized systems, a high interfacial irradiated surface area of the catalyst can be maintained despite its immobilization due to the large surface-to-volume ratio of the microchannels.

Photomicroreactors will remain an active area of research in the future, especially if interesting industrial applications can be identified by the fine chemical and pharmaceutical industries that make use of their described advantages.

References

1 K.-H. Pförtner, in *Ullmann's Encyclopedia of Industrial Chemistry,* 6th edn, Wiley-VCH, Weinheim, Germany, **2002**, Vol. *26*, p. 245.

2 P. Watts, C. Wiles, Recent advantages in synthetic micro reaction technology, *Chem. Commun.* **2007**, 443–476.

3 H. Lu, M.A. Schmidt, K.F. Jensen, Photochemical reactions and on-line UV detection in microfabricated reactors, *Lab Chip* **2001**, *1*, 22–28.

4 H. Maeda, H. Mukae, K. Mizuno, Enhanced efficiency and regioselectivity of intermolecular ($2\pi + 2\pi$) photocycloaddition of 1-cyanonaphthalene derivatives using microreactors, *Chem. Lett.* **2005**, *34*, 66–67.

5 H. Mukae, H. Maeda, S. Nashihara1, K. Mizuno, Intramolecular photocycloaddition of 2-(2-alkenyloxymethyl)naphthalene-1-carbonitriles using glass-made microreactors, *Bull. Chem. Soc. Jpn.* **2007**, *80*, 1157–1161.

6 T. Fukuyama, Y. Hino, N. Kamata, I. Ryu, Quick execution of [2 + 2] type photochemical cycloaddition reactions by a continuous flow system using a glass-made microreactor, *Chem. Lett.* **2004**, *33*, 1430.

7 A. Sugimoto, Y. Sumino, M. Takagi, T. Fufuyama, I. Ryu, The Barton reaction using a microreactor and black light. Continuous-flow synthesis of a key steroid intermediate for an endothelin receptor antagonist, *Tetrahedon Lett.* **2006**, *47*, 6197–6200.

8 D. Daniel, I.G.R. Gutz, Microfluidic cell with a TiO_2-modified gold electrode irradiated by an UV-LED for *in situ* photocatalytic decomposition of organic matter and its potentiality for voltammetric analysis of metal ions *Electrochem. Commun.* **2007**, *9*, 522–528.

9 S. Meyer, D. Tietze, S. Rau, B. Schäfer, G. Kreisel, Photosensitized oxidation of citronellol in microreactors, *J. Photochem. Photobiol. A* **2007**, *186*, 248–253.

10 R.C.R. Wootton, R. Fortt, A.J. de Mello, A microfabricated nanoreactor for safe, continuous generation and use of singlet oxygen, *Org. Process Res. Dev.* **2002**, *6*, 187–189.

11 H. Ehrich, D. Linke, K. Morgenschweis, M. Baerns, K. Jähnisch, Application of microstructured reactor technology for the photochemical chlorination of alkylaromatics, *Chimia* **2002**, *56*, 647–653.

12 K. Jähnisch, Photochemische Erzeugung und [4 + 2] Cycloaddition von Singulett-Sauerstoff im Mikrofallfilmreaktor, *Chem. Ing. Tech.* **2004**, *76*, 630–632.

13 K. Ueno, F. Kitagawa, N. Kitamura, Photocyanation of pyrene across an oil/water interface in a polymer microchannel chip, *Lab Chip* **2002**, *2*, 231–234.

14 R. Gorges, S. Meyer, G. Kreisel, Photocatalysis in microreactors, *J. Photochem. Photobiol. A* **2004**, *167*, 95–99.

15 N. Kitamura, K. Yamada, K. Ueno, S. Iwata, Photodecomposition of phenol by silica-supported porphyrin derivative in polymer microchannel chips, *J. Photochem. Photobiol. A* **2006**, *184*, 170–176.

16 Y. Matsushita, S. Kumada, K. Wakabayashi, K. Sakeda, T. Ichimura, Photocatalytic reductions in microreactors, *Chem Lett.* **2006**, *35*, 410–411.

17 Y. Matsushita, K. Sakeda, T. Suzuki, T. Ichimura, K. Tanibata, T. Murata, Multiphase photocatalytic reactions in microreactors, presented at the 1st European Chemistry Congress, 27–31 August **2006**, Budapest.

18 B. Choi, L. Xu, H.T. Kim, D.W. Bahnemann, Photocatalytic characteristics on sintered slass and micro reactor, *J. Ind. Eng. Chem.* **2006**, *12*, 663–672.

19 H. Lindstrom, R. Wootton, A. Iles, High surface area titania photocatalytic microfluidic reactors, *AIChE J.* **2007**, *53*, 695–702.

20 S. Teekateerawej, J. Nishino, Y. Nosaka, Design and evaluation of photocatalytic

micro-channel reactors using TiO_2-coated porous ceramics, *J. Photochem. Photobiol. A* **2006**, *179*, 263–268.

21 T. Kitamori, G. Takei, H.B. Kim, Photocatalytic redox-combined systhesis of L-pipecolinic acid with titania modified microchannel chip, *Catal. Commun.* **2005**, *6*, 357–360.

22 H. Míguez, F. Meseguer, C. López, Á. Blanco, J.S. Moya, J. Requena, A. Mifsud, V. Fornés, Control of the photonic crystal properties of fcc-packed submicrometer SiO_2 spheres by sintering, *Adv. Mater.* **1998**, *10*, 480.

23 H. Nakamura, X. Li, H. Wang, M. Uehara, M. Miyazaki, A simple method of self assembled nano-particles deposition on the micro-capillary inner walls and the reactor application for photocatalytic and enzyme reactions, *Chem Eng J.*, **2004**, *101*, 261–268.